EFFECT OF SPARSE-BUILD INTERNAL STRUCTURE ON PERFORMANCE OF FUSED DEPOSITION MODELING TOOLS UNDER PRESSURE

S. Meng, L. Mason, G. Taylor, X. Wang, M. C. Leu, and K. Chandrashekhara
Department of Mechanical and Aerospace Engineering
Missouri University of Science and Technology, Rolla, MO 65409

M. Matlack and J. Castle
The Boeing Company, St Louis, MO, 63134

Abstract

Two different approaches to design a sparse-build tool for fabrication by the fused deposition modeling (FDM) process are compared. One approach uses a 2D lattice structure and the other approach is inspired by topology optimization. Ultem 9085 is used as the material, and the amount of material used to build the tool is kept constant to ensure a fair comparison. A solid tool is also included in the comparison. The performance of the tool under uniform pressure is simulated using finite element analysis (FEA) and the accuracy of the FEA results is verified by comparing them with experimentally measured data for a similar tool. The build material, support material, build time, maximum displacement, and maximum von Mises stress are compared for the three build approaches, with an emphasis on the pros and cons of each sparse-build tool with regards to performance under uniform pressure and fabrication by FDM.

Introduction

Shortening the product development cycle time is a key factor in ensuring that a company remains ahead of its competitors. Additive manufacturing is a method of rapidly and efficiently fabricating a physical part based upon a design model, and it has been in use throughout various industries over the past three decades [1]. One of the major advantages of additive manufacturing is that the build time for product development is shortened significantly. Furthermore, additive manufacturing enables light-weight parts to be manufactured by changing the internal structure of the model from solid to sparse [2].

Additive manufacturing is a process where layers of material are formed and added to create three-dimensional parts. One of the processes for additive manufacturing is Fused Deposition Modeling (FDM). In this process, the material filament is heated just above the melting point and extruded through a nozzle to form the layers. Materials for FDM include: thermoplastics such as ABS, Ultem 9085, Ultem 1010, polycarbonate, and many others [3]. The FDM machines used to fabricate these parts offer a variety of customizable build parameters including: build direction, raster angle, raster width, raster air gap, wall/contour thickness, and cap thickness.

Topology optimization has become an important research area in structural design. It utilizes a mathematical approach that optimizes material distribution within a desired design space. The optimization is based on an objective function with constraints in response to a set of loads and boundary conditions [4]. The most common objectives used in topology optimization

are the minimization of compliance or mass. Additional constraints, such as maximum allowable stress or displacement, can be added to direct the optimization process and produce even more desirable results. The topology optimization software used for this study, solidThinking Inspire 2015, utilizes the SIMP method along with a mass/volume filter. Topology optimization works with an existing CAD model to help design structural parts and has the ability to reduce the cost, development time, material usage, and weight of a product.

Finite element analysis is widely used to model additive manufacturing processes. However, literature data on modeling and simulation of FDM parts is still limited. Zhang and Chou [5] constructed a thermo-mechanical finite element model to simulate stress accumulation and the distortion of parts during the filament deposition process. Miquel *et al.* [6] built an effective finite element model which was based on tension tests performed on FDM parts. This verified finite element model can predict proper material orientations under varying loading conditions. Mostatfa *et al.* [7] used ANSYS to simulate ABS-iron composite FDM manufacturing process including various build parameters. Li *et al.* [8] developed a finite element model to simulate the vacuum assisted resin transfer molding process for composites with molds manufactured with the FDM process. The FDM part was optimized based on this verified finite element model. Finite element analysis has shown to be an effective method to study and optimize FDM parts.

In the current study, a tool with geometry based on composite molding tools is investigated for the effects of replacing the interior of the tool with sparse-build internal structures. Two different sparse-build internal structures are used: a 2D lattice structure called sparse double dense (SDD) and a topology optimization inspired (TOI) design. To ensure the comparability, the material volumes of the SDD and TOI tools are kept the same. A tool with a solid internal structure is used as a reference in the comparison. The performance of the tool under uniform pressure is simulated using FEA. The accuracy of the FEA results is verified by comparing them with experimentally measured data for a similar tool. The build material, support material, build time, maximum displacement, and maximum von Mises stress are compared for the three build approaches.

Tool Geometry and Internal Structure Generation
Tool Geometry
The geometry of the tool used for this study is shown in Figure 1a. It is a square plate with a curved top surface. An illustration of the uniform pressure loading condition is shown in Figure 1b. The model has a uniform pressure load of 0.6895 MPa on all surfaces except the bottom surface, where a rigid flat plate provides the boundary conditions. This geometry and loading condition are based off of common composite molding tools.
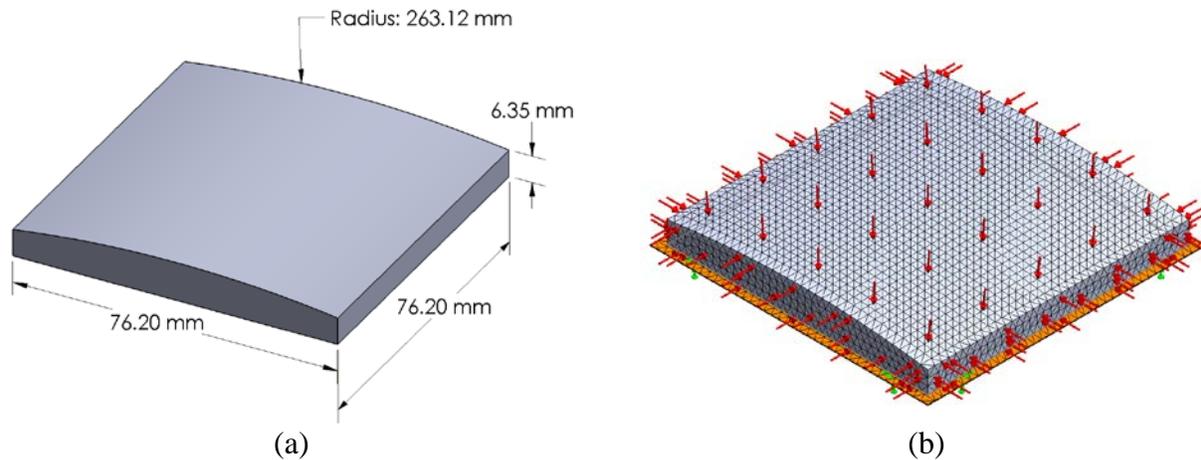
Figure 1: (a) Tool geometry and (b) loading condition

Sparse Double Dense Design

Sparse double dense (SDD) is a light weight internal structure commonly used in FDM tooling and manufacturing applications. This internal structure has the advantages of a reduced amount of build material, shorter build time, and higher strength-to-mass ratio compared to a solid internal structure. The SDD parameters used in this study are shown in Figure 2. The raster air gap and raster angle are kept at the default values of 2.032 mm and 45 degrees, respectively. A single contour, or layer outline, is chosen instead of multiple contours to minimize the effect of the contour on the study of the internal structure. Since the extrusion tip, T16, is capable of widths from 0.4064 mm to 0.7620 mm, a raster width closest to the midpoint is chosen at 0.6096 mm.
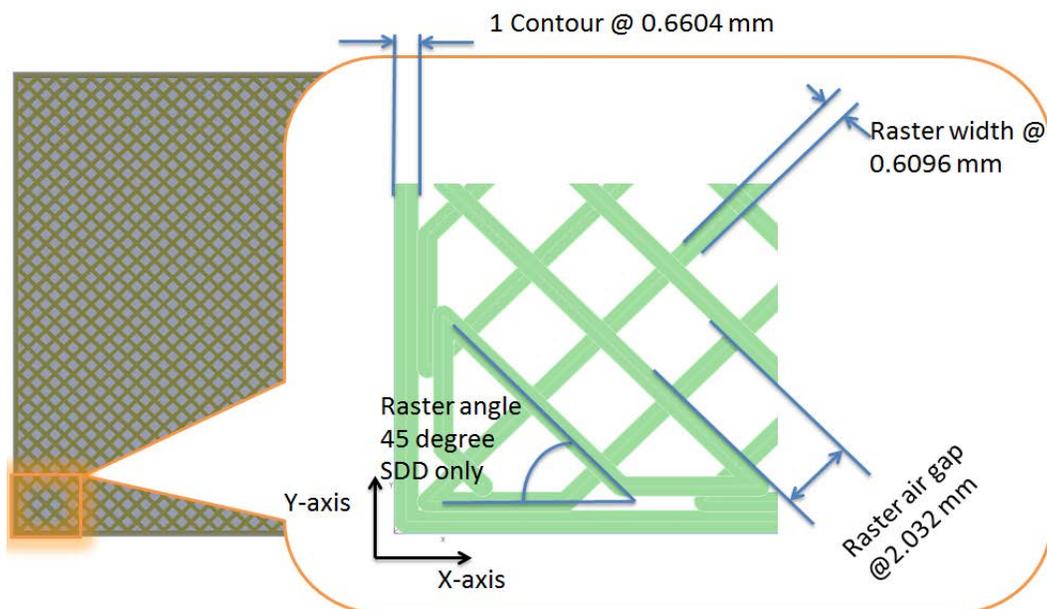

Figure 2: Sparse double dense cross section and parameters

Topology Optimization Inspired Design

The topology optimization design is conducted using Altair HyperWorks solidThinking Inspire 2015. This software can perform optimizations using two different objectives: minimize mass or maximize stiffness. For the minimize-mass objective, there is an optional minimum safety factor constraint. For the maximize-stiffness objective, there is an optional mass target constraint where the user can specify the target mass as a percentage of the design space or as a total mass value. In this study, the maximize-stiffness objective is used and the mass target is specified as a total mass value equaling that of the SDD tool.

Topology optimization has a mesh dependency, meaning that different mesh densities affect the results. Due to this dependency, denser meshes create more intricate topology optimization results. As shown in Figure 3, the topology optimization study is completed with four different mesh densities governed by the average tetrahedral element size: low (10.16 mm), mid-low (5.08 mm), mid-high (2.54 mm), and high (1.15 mm).
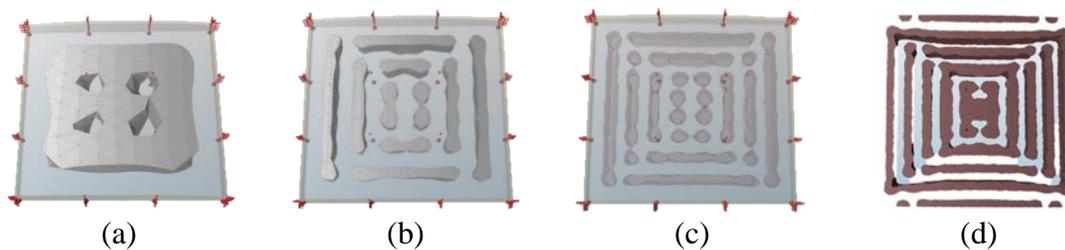

(a)　　　　　　(b)　　　　　　(c)　　　　　　(d)

Figure 3: Cross sections of topology optimization results with four different mesh densities governed by the average tetrahedral element size: (a) low (10.16 mm), (b) mid-low (5.08 mm), (c) mid-high (2.54 mm), and (d) high (1.15 mm)

As the topology optimization results get more and more refined with increasing mesh density and number of elements, the run time for the optimization increases. The high mesh density optimization run takes over 24 hours to complete with an element size of 1.15 mm. In this study, run times longer than this are not feasible. The results shown in Figure 3 show the tendency for the topology optimization structure to split up into an increasing number of 0 and 90 degree walls as the mesh density increases. These walls can be connected together in such a way as to form nesting squares, or stiffeners, with a solid square in the middle as the smallest stiffener. Following this convention, the low mesh density (10.16mm) can be approximated by two square stiffeners, the mid-low (5.08mm) by three, the mid-high (2.54mm) by four, and the high (1.15mm) by five. It is logical that further increasing the mesh density for the topology optimization would result in an increasing number of these stiffeners. Inspired by this pattern of an increasing number of stiffeners, designs are created with 5, 10, 15, and 20 stiffeners, as shown in Figure 4.
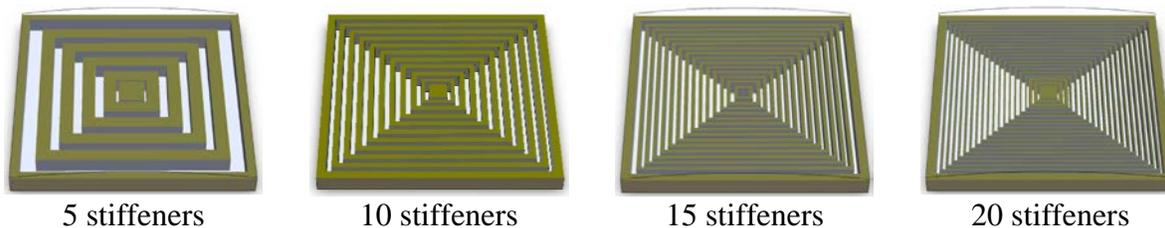

5 stiffeners　　　　10 stiffeners　　　　15 stiffeners　　　　20 stiffeners

Figure 4: Topology optimization inspired designs

Results and Discussion

An FEA study is run on the TOI tools shown in Figure 4 and the performance of the four tools are compared. The tool with 10 stiffeners has the lowest maximum von Mises stress and the lowest maximum displacement. To substantiate this finding and populate more data, TOI tools with 7, 8, 9, 11, 12, 13, and 17 stiffeners are modeled and included in the FEA study. The maximum von Mises stress and maximum resultant displacement results for the TOI tools are shown in Figure 5 and Figure 6, respectively. As the number of stiffeners increases, the maximum von Mises stress and the maximum displacement both decrease until they reach 10 stiffeners; at which point the maximum von Mises stress remains relatively constant and the maximum displacement starts increasing. Since minimizing the maximum displacement and maximum von Mises stress is desirable for this tool, the tool with 10 stiffeners is the logical choice based on the results. Therefore, the TOI tool with 10 stiffeners is chosen as the representative TOI tool and compared with the solid and SDD tools.
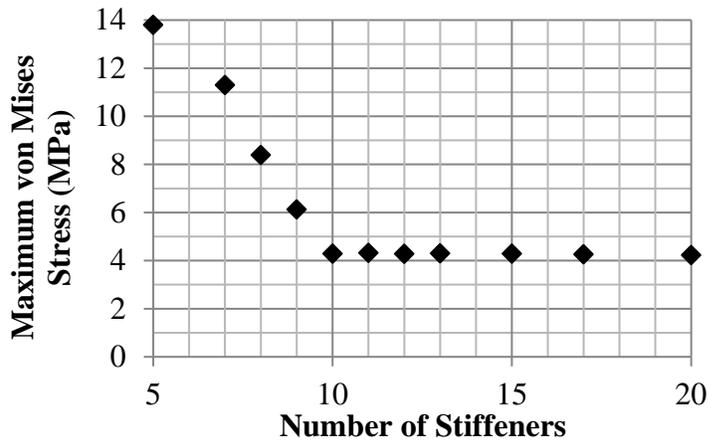
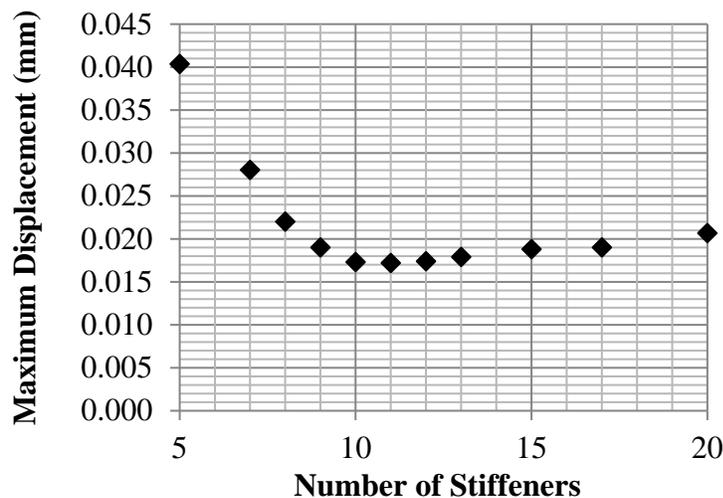Figure 5: Maximum von Mises stress of TOI tools

Figure 6: Maximum resultant displacement of TOI tools

The resultant displacement contour plots for the three tools are shown in Figure 7, where the three tools are oriented to show the top and front surfaces. The dark blue indicates the minimum displacement and the dark red the maximum displacement. The maximum resultant displacement occurs at the curved edges between the top surface and the front and back surfaces. These edges deform inward towards the middle of the tool during the simulation. The maximum resultant displacement of the SDD (0.0118 mm) and TOI (0.0173 mm) tools are an order of magnitude larger than the solid tool (0.00148 mm). The resultant displacements along the sides of the solid and SDD tools are fairly constant along the length. This suggests that the SDD tool deforms in a manner very similar to the solid tool. The TOI tool, however, has a distinctly different deformation pattern. The areas of minimum resultant displacement on the top surface of the TOI tool run along the diagonals of the square instead of the side edges like the other tools. Additionally, the green (0.0072 mm - 0.0101 mm) areas of the TOI tool correspond to the same magnitude of deflection as the yellow to red (0.0070 mm – 0.0118 mm) areas on the SDD tool. Clearly, the TOI tool is not able to maintain its shape as well as the SDD tool.

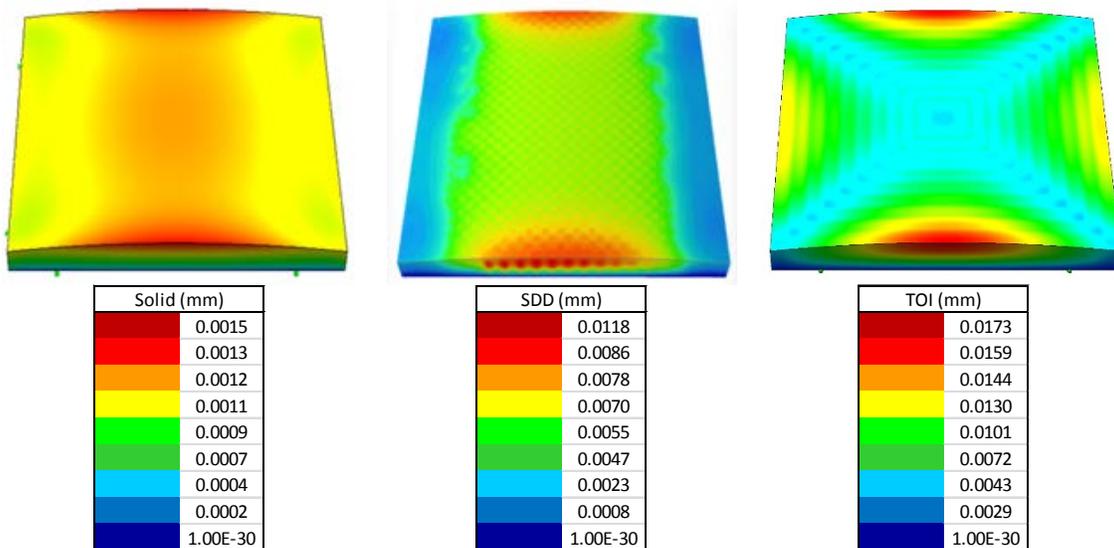| Solid (mm)		SDD (mm)		TOI (mm)	
	0.0015		0.0118		0.0173
	0.0013		0.0086		0.0159
	0.0012		0.0078		0.0144
	0.0011		0.0070		0.0130
	0.0009		0.0055		0.0101
	0.0007		0.0047		0.0072
	0.0004		0.0023		0.0043
	0.0002		0.0008		0.0029
	1.00E-30		1.00E-30		1.00E-30

Figure 7: Resultant displacement contour plots

Another displacement issue to consider is the appearance of dimpling. The z-axis displacement contour plots are shown in Figure 8. The dark blue indicates the maximum negative (downwards) displacement and the dark red the maximum positive (upwards) displacement. Both sparse-build tools show their internal support structure clearly in these diagrams. The light blue shows where the shell is supported and the dark blue shows where depressions in the shell have formed, called dimples. The magnitude of the dimpling can be described as the difference between the maximum displacement of an unsupported area and the minimum displacement of the supported areas that are directly adjacent. The dimpling magnitude can be roughly estimated from Figure 8 to be 0.001 mm for the SDD tool and 0.002 mm for the TOI tool. The SDD tool has a smaller maximum displacement and less significant dimpling than the TOI tool.
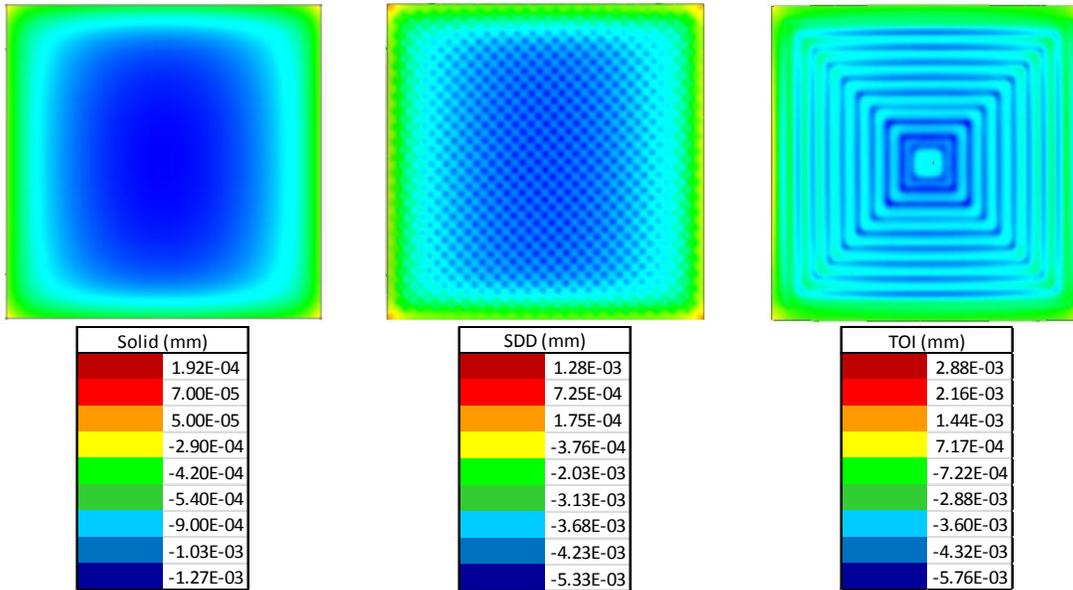
Figure 8: Z-axis displacement contour plots

The amount of build material, support material, and build time for each tool are estimated using the Insight 10.2 and Control Center 10.2 software. This software is created by Stratasys specifically for their machines. Insight allows the user to process individual STL files by slicing them into layers, placing support material, creating tool paths for each layer, and then sending a CMB file with that information to the Control Center. The Control Center then allows the user to configure the placement of one or more CMB files on the build platform, estimates the amount of build material, support material, and time required to build the parts, and sends the information to the machine. Table 1 shows the estimated tool fabrication requirements as well as the maximum resultant displacement and maximum von Mises stress from the FEA study. Figure 9 shows a side by side comparison of the results from Table 1.

The SDD and TOI tools require the same amount of build material, 64% of the solid tool. The solid and SDD tools require no support material besides the base that each part is printed on, but the TOI tool requires 8.35 cm^3 of support material inside the tool to support the top shell in between the stiffeners. This poses a problem as the support material inside the TOI tool cannot be removed and would affect the performance of the tool. Since the properties of the support material are not given, it is not possible to include this in the FEA study.

Table 1: Estimated tool fabrication requirements and FEA results

	Build Material (cm^3)	Support Material (cm^3)	Build Time (min)	Maximum Resultant Displacement (mm)	Maximum von Mises Stress (MPa)
Solid	44.41	1.64	48	0.00148	0.75
SDD	28.35	1.64	35	0.0118	4.51
TOI	28.35	9.99	111	0.0173	4.29

The SDD tool is expected to have a shorter build time than the solid tool and the results are consistent with this expectation. As far as fabrication goes, the only differences between solid and SDD are the raster air gap (which is zero for solid parts) and the number of extrusions per layer. Increasing the raster air gap not only decreases the amount of material, it also decreases the number of times the nozzle has to go back and forth to fill the layers, thus decreasing the build time. The TOI tool, on the other hand, has a complicated internal geometry compared to the other tools. For most of the layers, each solid area in the cross section requires 2-4 extrusions to create, and each area filled with support material requires at least 2 extrusions. That takes a minimum of 62 extrusions for the most complicated layers of the TOI tool, compared to a maximum of 3 extrusions for SDD and 2 for solid. Every time the nozzle switches between the build material and support material, it pauses to change the temperature of the heating element that melts the material. These pauses add a lot of time to the total build time, making the TOI tool take over three times as long to build as the SDD tool. However, if the TOI tool is built without support material, the build time would be about the same as the solid tool, which suggests that transitioning from one material to the other and back again for each layer increased the build time by over 130%.
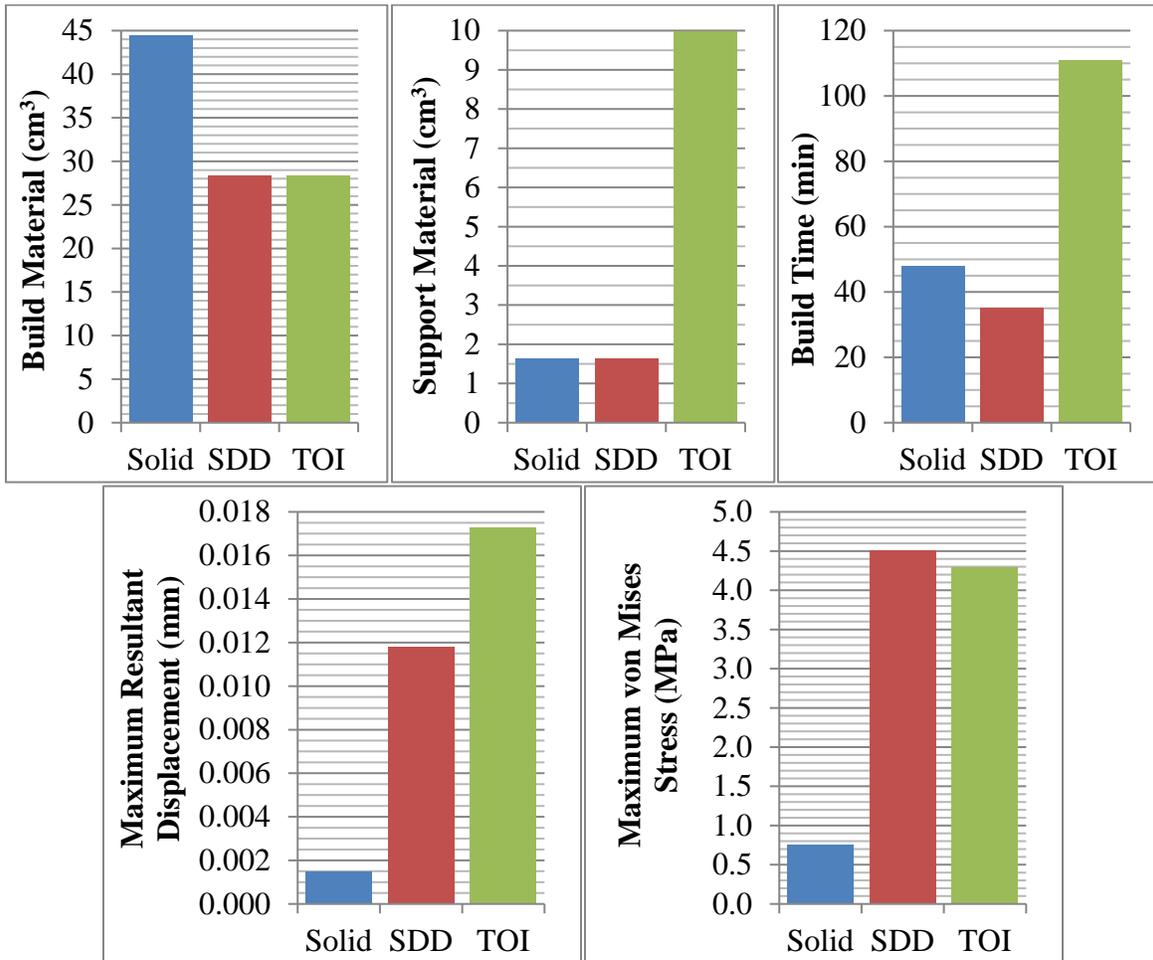

Figure 9: Results comparison

The compressive yield strength of Ultem 9085 is 87-100 MPa, depending on the orientation of the load with respect to the print direction. Using the lower bound of the compressive yield strength range, the tools have a factor of safety of 116 for the solid tool, 19 for the SDD tool, and 20 for the TOI tool. All three tools can safely withstand the 0.6895 MPa pressure load.

Experimental Verification

Since the uniform pressure loading condition cannot be experimentally tested for this study, an FEA study is performed to simulate the uniform pressure results. To ensure the accuracy of the results for the original tool, an FEA study is run on a verification tool and the results are compared to a compression test experiment. The machine used for the compression testing is an INSTRON 5985. The verification tool is a modified version of the original tool geometry in this study. As shown in Figure 10, the verification tool has a flat top to create a uniform distributed load on the top of the tool during the compression test.
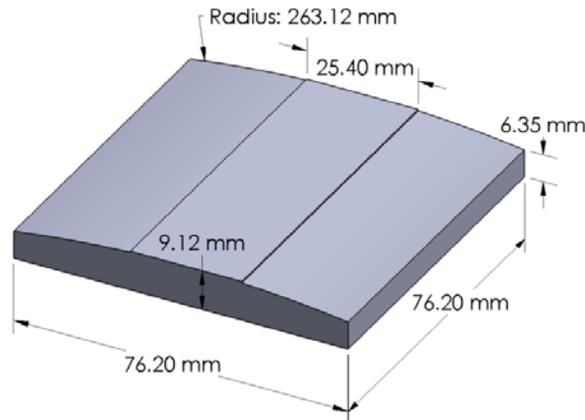

Figure 10: Verification tool geometry

The SDD internal structure is applied and a topology optimization is performed on the verification tool in the same manner as the original tool. The topology optimization result is shown in Figure 11, which is then modified to have a single flat vertical surface on either side instead of the triangular mesh surface.
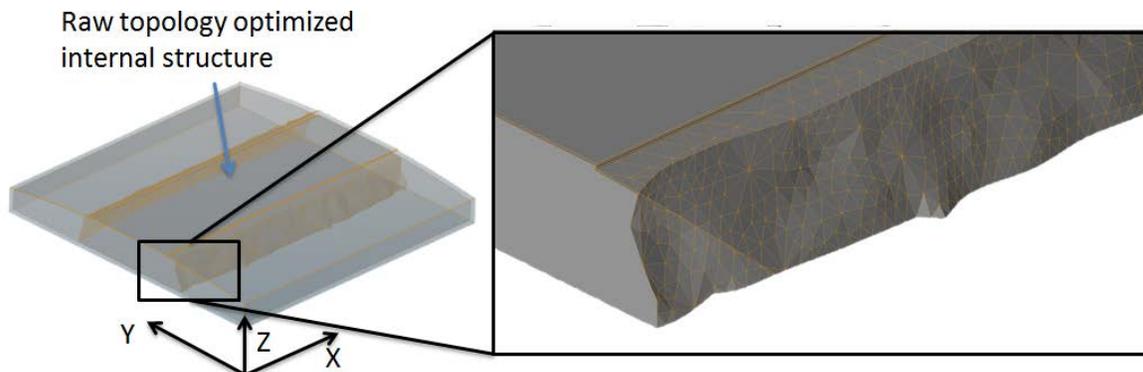

Figure 11: Topology optimization result for the verification tool

The verification tools are fabricated using a Stratasys Fortus 400mc machine with Ultem 9085 as the print media. Five samples each of the solid, SDD, and topology optimized verification tools are fabricated and then compression tested. The experimental and FEA results are shown in Figure 12. The difference between the FEA and experimental results are 0.45% for solid, 7.66% for SDD, and 6.16% for topology optimization (TO). The results are in good agreement; therefore the accuracy of the FEA results is verified.
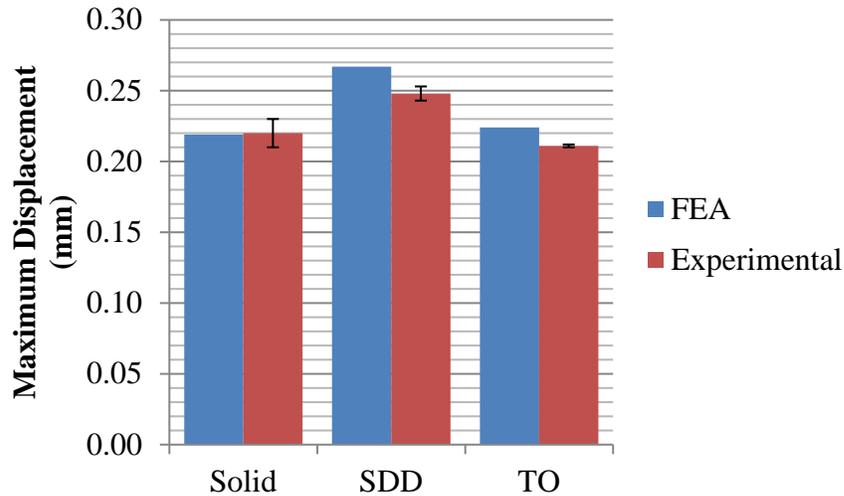

Figure 12: Verification tool results

Conclusion

A tool, with the geometry and loading condition based off of composite molding tools, is investigated for the effects of replacing the interior of the tool with two sparse-build internal structures: sparse double dense (SDD) and a topology optimization inspired (TOI) design. The performance of the tool under uniform pressure is simulated using FEA.

The maximum resultant displacements of the SDD (0.0118 mm) and TOI (0.0173 mm) tools are an order of magnitude larger than that of the solid tool (0.00148 mm). The build material for the SDD and TOI tools are kept constant at 64% of the solid tool. The TOI tool requires interior support material, which increases the build time by over 130% and cannot be removed. The tools have a factor of safety of 116 for the solid tool, 19 for the SDD tool, and 20 for the TOI tool. Thus all three tools can safely withstand the 0.6895 MPa pressure load.

For the composite molding application of this tool, the outer surface displacement has the greatest impact on the quality of the composite product. It stands to reason that the SDD tool would produce a higher quality product than the TOI tool as it has a lower maximum displacement, less significant dimpling, and a similar displacement pattern to the solid tool. The SDD tool is also the logical choice when additive manufacturing is taken into consideration since it has the shortest build time and requires no extra support material. The TOI tool has a slightly lower maximum von Mises stress than the SDD tool, but this advantage can be considered negligible due to the excessively large factor of safety. Therefore, for this study the SDD internal structure is more desirable than the TOI internal structure.

Acknowledgements

References

[1] C. K. Chua, K. F. Leong, and C. S. Lim, Rapid Prototyping: Principles and Applications, vol. 1, 2nd ed. Singapore, Singapore: World Scientific Publishing Co Pte, 2003, pp. 124–129.

[2] O. Iyibilgin, M. C. Leu, G. Taylor, H. Li, and K. Chandrashekhara, "Investigation of Sparse-Build Rapid Tooling by Fused Deposition Modeling," in *Solid Freeform Fabrication Symposium*, 2014.

[3] N. Guo and M. C. Leu, "Additive manufacturing: Technology, applications and research needs," Frontiers of Mechanical Engineering, vol. 8, no. 3, pp. 215–243, May 2013.

[4] M. P. Bendsøe and O. Sigmund, Topology optimization: Theory, methods and applications, 2nd ed. New York: Springer-Verlag Berlin and Heidelberg GmbH & Co. K, 2002.

[5] Y. Zhang and Y. K. Chou, "Three-dimensional finite element analysis simulations of the fused deposition modelling process," Proceedings of the Institution of Mechanical Engineers, Part B: Journal of Engineering Manufacture, vol. 220, no. 10, pp. 1663–1671, Jan. 2006.

[6] M. Domingo-Espin, J. M. Puigoriol-Forcada, A. Garcia-Granada, J. Llumà, S. Borros, and G. Reyes, "Mechanical property characterization and simulation of fused deposition modeling Polycarbonate parts," Materials & Design, vol. 83, pp. 670–677, Oct. 2015.

[7] N. Mostafa, H. M. Syed, S. Igor, and G. Andrew, "A study of melt flow analysis of an ABS-Iron composite in fused deposition modelling process," Tsinghua Science and Technology, vol. 14, no. S1, pp. 29–37, Jun. 2009.

[8] H. Li, G. Taylor, V. Bheemreddy, O. Iyibilgin, M. C. Leu, and K. Chandrashekhara, "Modeling and characterization of fused deposition modeling tooling for vacuum assisted resin transfer molding process," Additive Manufacturing, vol. 7, pp. 64–72, Jul. 2015.